JACS
JOURNAL OF THE AMERICAN CHEMICAL SOCIETY

Subscriber access provided by ISTANBUL TEKNIK UNIV

Article

Hierarchical Self-Assembly of Aminopyrazole Peptides into Nanorosettes in Water

Petra Rzepecki, Katrin Hochdrffer, Torsten Schaller, Jan Zienau, Klaus Harms, Christian Ochsenfeld, Xiulan Xie, and Thomas Schrader

J. Am. Chem. Soc., **2008**, 130 (2), 586-591 • DOI: 10.1021/ja0744807

Downloaded from http://pubs.acs.org on February 8, 2009

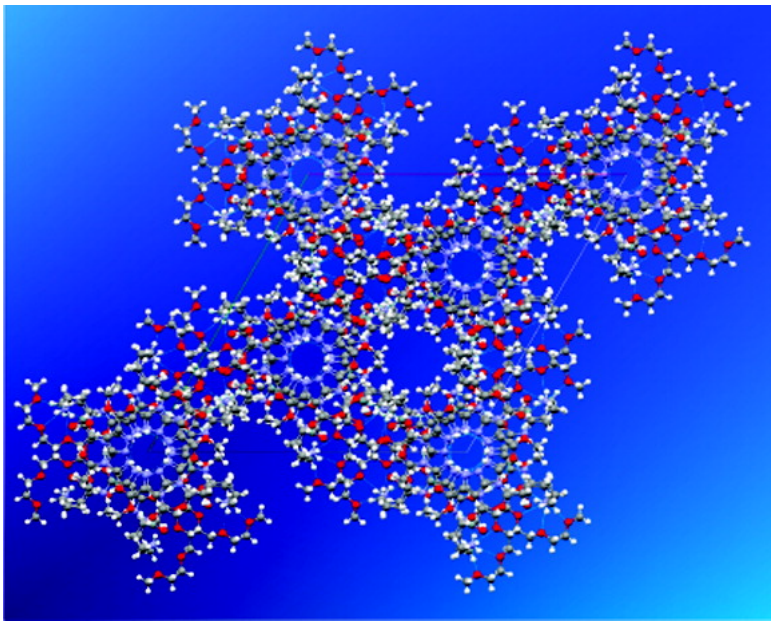

More About This Article

Additional resources and features associated with this article are available within the HTML version:

- Supporting Information
- Links to the 1 articles that cite this article, as of the time of this article download
- Access to high resolution figures
- Links to articles and content related to this article
- Copyright permission to reproduce figures and/or text from this article

View the Full Text HTML

ACS Publications
High quality. High impact.

Journal of the American Chemical Society is published by the American Chemical Society. 1155 Sixteenth Street N.W., Washington, DC 20036

J|A|C|S
ARTICLES
Published on Web 12/14/2007

Hierarchical Self-Assembly of Aminopyrazole Peptides into Nanorosettes in Water

Petra Rzepecki,[†] Katrin Hochdörffer,[†] Torsten Schaller,[†] Jan Zienau,[‡] Klaus Harms,[§] Christian Ochsenfeld,*[,‡] Xiulan Xie,*[,§] and Thomas Schrader*[,†]

Institute of Organic Chemistry, Universität Duisburg-Essen, Universitätsstrasse 5, 45117 Essen, Germany, Institute of Physical and Theoretical Chemistry, Universität Tübingen, Auf der Morgenstelle 8, 72076 Tübingen, Germany, and Department of Chemistry, Philipps-Universität Marburg, Hans-Meerwein-Strasse, 35032 Marburg, Germany

Received July 13, 2007; E-mail: Thomas.Schrader@uni-due.de

Abstract: Self-association of aminopyrazole peptide hybrid **1** leads to stacked nanorosettes. This remarkable, well-ordered structure obeys the laws of nucleic acid self-assembly. In a strictly hierarchical process, formation of aminopyrazole "base" triplets via a hydrogen bond network is accompanied by π-stacking with a second rosette and final dimerization of two double rosettes to a four-layer superstructure, stabilized by a six-fold half-crown alkylammonium lock. The final complex is soluble in organic as well as in aqueous solution. It was characterized in the solid state by X-ray crystallography, in water by NMR spectroscopy, and *in silico* by quantum chemical shift calculation. All these methods provide strong evidence for the same hexameric complex geometry. Its structural features bear striking silimarity to nucleic acid architectures and their peptidic counterparts, especially alanyl-PNA. The whole self-assembly process is highly solvent- and temperature-dependent and occurs with a high degree of cooperativity—no intermediates are observed. Formation and dissociation of the nanorosette, however, are kinetically slow. The limitation to a hexameric aggregate can be explained by six sterically demanding valine residues, whose replacement by alanines may result in formation of infinite fibers.

Introduction

The factors governing self-assembly processes of nucleic acids, although intensely investigated, are still under debate.[1] A fundamental architectural principle is the typical combination of two-dimensional hydrogen bond recognition (base pairs) with one-dimensional π-stacking (helix) of several planes. Thus, pairing specificity, according to the classical view, is achieved through hydrogen bonding and stability by stacking. The fascinating self-assembly process of nucleic acids, with its fundamental importance for life on earth, has spurred numerous investigations on model compounds. Imitating the G quartet motif,[2] found in nature, Whitesides was able to produce an entirely artificial supramolecular rosette, which spontaneously self-assembled in chloroform from melamine and cyanuric acid components.[3] Reinhoudt et al. attached two melamine units onto calixarenes and created preorganized building blocks capable of forming stacked double rosettes with cyanuric acids and barbiturates in organic solvents. 15-Component tetrarosette associates, held together by 72 hydrogen bonds, could be created in quantitative yield.[4] These had remarkable properties, such as supramolecular chirality and memory effects.[5] Using the DDA/ADD motif, Zimmerman et al. designed a more robust hexameric, disk-shaped aggregate, which was stable in 8% aqueous tetrahydrofuran (THF).[6] Meijer et al. created highly stable quadruply hydrogen-bonded dimers from self-complementary bifunctionalized heterocyclic units connected by a spacer, which spontaneously self-assemble into columnar polymeric architectures.[7] It was claimed that in water, stacking of the hydrogen-bonded pairs leads to hydrophobic microdomains, allowing cooperative hydrogen bonding.[8] A related approach has before been described by the Lehn group, who achieved a molecular-recognition-directed helical polyassociation of complementary components, mimicking DNA self-assembly, albeit in chloroform.[9] Fenniri et al. balanced enthalpic loss (hydrogen

[†] Universität Duisburg-Essen.
[‡] Universität Tübingen.
[§] Philipps-Universität Marburg.

(1) (a) Saenger, W. *Principles of Nucleic Acid Structure*; Springer: New York, 1984. (b) Eschenmoser, A.; Loewenthal, E. *Chem. Soc. Rev.* **1992**, *21*, 1−16. (c) Detmer, I.; Summerer, D.; Marx, A. *Chem. Commun.* **2002**, 2314−2315.
(2) Related folic acid quartets: Gottarelli, G.; Mezzina, E.; Spada, G. P.; Carsughi, F.; di Nicola, G.; Mariani, P.; Sabatucci, A. *Helv. Chim. Acta* **1996**, *79*, 220−234. See also: Davis, J. T.; Spada, G. P. *Chem. Soc. Rev.* **2007**, *36*, 296−313. Davis, J. T. *Angew. Chem., Int. Ed.* **2004**, *43*, 668−698.
(3) Mathias, J. P.; Seto, C. T.; Simanek, E. E.; Whitesides, G. M. *J. Am. Chem. Soc.* **1994**, *116*, 1725−1736; 4326−4340.
(4) Jolliffe, K. A.; Timmerman, P.; Reinhoudt, D. N. *Angew. Chem., Int. Ed.* **1999**, *38*, 933−937.
(5) Prins, L. J.; Huskens, J.; de Jong, F.; Timmerman, P.; Reinhoudt, D. N. *Nature* **1999**, *398*, 498−502. Prins, L. J.; de Jong, F.; Timmerman, P.; Reinhoudt, D. N. *Nature* **2000**, *408*, 181−84. ten Cate, M. G. J.; Omerovic, M.; Oshovsky, G. V.; Crego-Calama, M.; Reinhoudt, D. N. *Org. Biomol. Chem.* **2005**, *3*, 3727−3733.
(6) Kolotuchin, S. V.; Zimmerman, S. C. *J. Am. Chem. Soc.* **1998**, *120*, 9092−9093.
(7) Ky Hirschberg, J. H. K.; Brunsveld, L.; Ramzi, A.; Vekemans, J. A. J. M.; Sijbesma, R. P.; Meijer, E. W. *Nature* **2000**, *407*, 167−170.
(8) Brunsveld, L.; Vekemans, J. A. J. M.; Hirschberg, J. H. K. K.; Sijbesma, R. P.; Meijer, E. W. *Proc. Natl. Acad. Sci. U.S.A.* **2002**, *99*, 4977−4982.
(9) Gulik-Krzywicki, T.; Fouquey, C.; Lehn, J. M. *Proc. Natl. Acad. Sci. U.S.A.* **1993**, *90*, 163−167.

10.1021/ja0744807 CCC: $40.75 **© 2008 American Chemical Society**

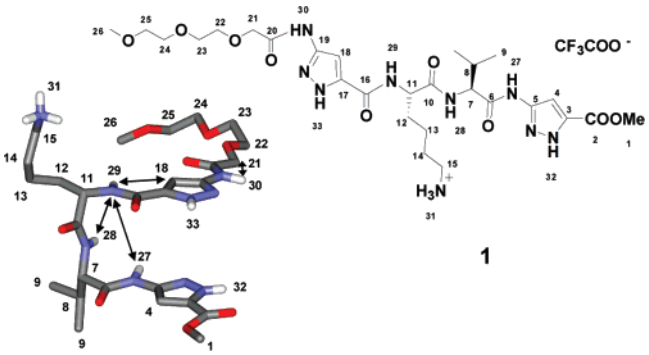

Figure 1. Lewis structure of hybrid peptide **1** and its conformation in the crystal, which is in accordance with Karplus analysis and NOE contacts found in aqueous solution. Double arrows indicate reciprocal intramolecular cross-peaks of a ROESY experiment in water at 298 K.

bonds) with entropic gain (stacking and hydrophobic effect) and created a self-assembling module possessing the Watson−Crick patterns for guanine *and* cytosine in one annulated heterocycle (G∧C); these finally form rosette nanotubes in *water*, with entropically driven growth during annealing.[10] However, very few artificial rosette models are stable in water, and those which are did not furnish a crystal structure.

We recently discovered that a single aminopyrazole−amino acid hybrid peptide out of a larger series, originally planned as β-sheet ligands,[11] acts as a powerful self-organizing unit and produces what could be called the analogy of a stacked base triplet.[12] Specifically, a tetrapeptide from two aliphatic proteinogenic amino acids (Lys-Val), flanked by two heteroaromatic amino acids with an oligoethyleneglycol tether, avoids the extended conformation observed in all other members of this series (Figure 1). It forms instead a highly ordered, tightly packed structure in the solid state and in aqueous solution, shown independently by X-ray crystallography (solid state) and NMR experiments (solution), supplemented by quantum chemical calculations. This aminopyrazole peptide hybrid (**1**) self-assembles into aggregates with an obvious resemblance to nucleic acids, and the underlying principles may be utilized for the design of bio-inspired new materials with increasing complexity.

Results and Discussion

Crystals for an X-ray structure determination were grown from trifluoroacetic acid (TFA)/diethyl ether.[13] They reveal three levels of molecular recognition, comprising three major types of noncovalent interaction (Figure 2): (a) A planar network of hydrogen bonds is formed between three aromatic N-terminal amino acids, forming a pyrazole rosette. This is, in fact, a well-known self-association motif,[14] but here it is reinforced by four interconnecting hydrogen bonds between each heterocycle and its partners.[15] (b) A double kink in the bridging dipeptide unit

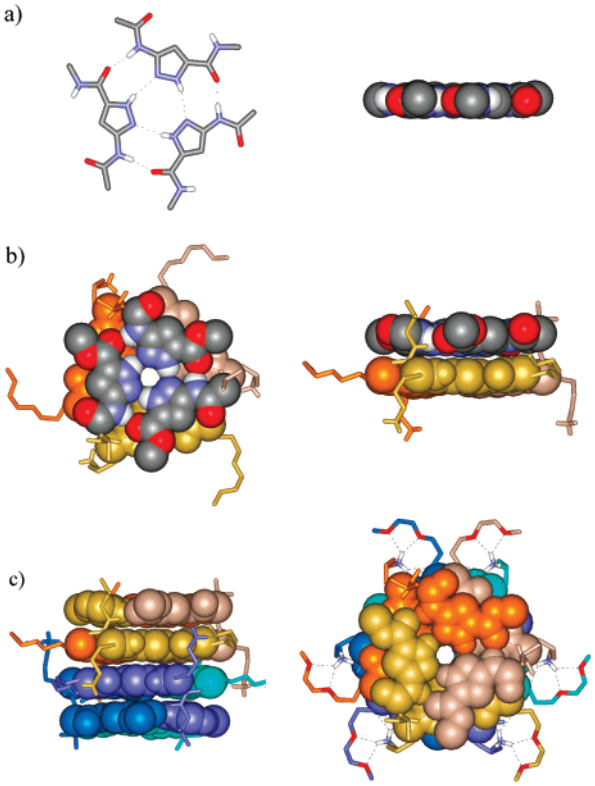

Figure 2. Segments of the crystal structure of **1**, demonstrating the three hierarchical levels of self-assembly: pyrazole rosette, double rosette, and half-crown locks.

brings each heteroaromatic C-terminal amino acid into parallel orientation with respect to the N-terminal ones, leading to a second identical pyrazole rosette, at the perfect interplanar distance of 3.4 Å for extensive π-stacking interactions. (c) After π-face docking of two double-rosettes, lysine residues of one trimeric peptide unit insert into ethyleneglycol tails of another and thus establish a six-fold lock with crown-ether-type ammonium complexation by ionic hydrogen bonds. The crystal structure does not reveal the location of the six trifluoroacetate counterions: these remain either disordered or even mobile, similar to toluene molecules inside Reinhoudt's rosette.[16] This remarkable total counterion separation in organic solution indicates a high bonding energy of the half-crown motif. It should be emphasized that the hierarchical analysis of the noncovalent interactions which lead to the hexameric superstructure implies by no means that these appear in consecutive order. Without a detailed kinetic investigation, a mechanistic picture cannot be delineated at this stage.

The whole arrangement mimics the base pairs, triplets, or quartets of nucleic acids likewise held at an optimal 3.4 Å distance for efficient π-stacking interactions. Heterocyclic nuclei of two successive parallel planes are here stacked in such a way that their molecular dipoles attract each other.[17] This can be seen from semiempiric calculations (AM1) of the electrostatic potential surface (EPS, Figure 3).[18] Its color code also indicates an extensive charge neutralization upon hydrogen bonding,

(10) Fenniri, H.; Mathivanan, P.; Vidale, K. L.; Sherman, D. M.; Hallenga, K.; Wood, K. V.; Stowell, J. G. *J. Am. Chem. Soc.* **2001**, *123*, 3854. Fenniri, H.; Deng, B.-L.; Ribbe, A. E. *J. Am. Chem. Soc.* **2002**, *124*, 11064. Johnson, R. S.; Yamazaki, T.; Kovalenko, A.; Fenniri, H. *J. Am. Chem. Soc.* **2007**, *129*, 5735−5743.
(11) (a) Rzepecki, P.; Schrader, T. *J. Am. Chem. Soc.* **2005**, *127*, 3016−3025. (b) Rzepecki, P.; Geib, N.; Peifer, M.; Biesemeier, F.; Schrader, T. *J. Org. Chem.* **2007**, *72*, 3614−3624.
(12) Related stacked triplexes: Lehn, J.-M. *J. Am. Chem. Soc.* **1998**, *120*, 9526−0532. Bocher, E.; Simard, M.; Wuest, J. D. *J. Org. Chem.* **1995**, *60*, 1408−1412. Zimmerman, S. C.; Duerr, B. F. *J. Org. Chem.* **1992**, *57*, 2215.
(13) Supplementary crystallographic data: CCDC 638569.
(14) Klein, O.; Aguilar-Parrilla, F.; Lopez, J. M.; Jagerovic, N.; Elguero, J.; Limbach, H.-H. *J. Am. Chem. Soc.* **2004**, *126*, 11718−11732.
(15) Quadruple hydrogen-bonded systems: Sijbesma, R. P.; Meijer, E. W. *Chem. Commun.* **2003**, 5−16.
(16) Timmerman, P.; Vreekamp, R. H.; Hulst, R.; Verboom, W.; Reinhoudt, D. N.; Rissanen, K.; Udachin, K. A.; Ripmeester, J. *Chem. Eur. J.* **1997**, *3*, 1823−1832.
(17) Chessari, G.; Hunter, C. A.; Low, C. M. R.; Packer, M. J.; Vinter, J. G.; Zonta, C. *Chem. Eur. J.* **2002**, *8*, 2860−2867.

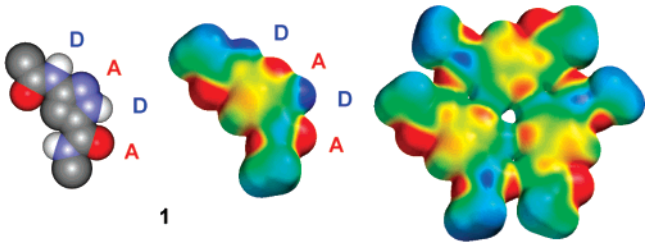

Figure 3. Electrostatic potential surface, calculated with AM1 for the core unit of **1** and its assembly into a single nanorosette (MEP color code: blue, +25 kcal/mol; red, −25 kcal/mol). Note the relatively even charge distribution after rosette formation.

producing a rosette of lower overall polarity, in accordance with the above-detailed stability considerations. Finally, π-stacking occurs mainly between hydrogen bond arrays and orthogonally placed pyrazole rings, as recently observed in a complex between 9-ethyladenine and an artificial receptor.[19]

At ambient temperature, the hybrid peptide is monomeric in a broad range of solvents, including water. To probe the self-association tendency in organic solution under crystallization conditions, a relatively concentrated solution was prepared in TFA (27 mM) and slowly cooled to 283 K. Only one set of signals was observed, which was examined by diffusion-ordered spectroscopy (DOSY) and shown to be the monomer. Subsequently, ether was titrated into the TFA solution until 30 vol % was reached, and a variable-temperature experiment was conducted until 223 K was reached (freeze point). The ^{1}H NMR spectrum remained unaltered throughout the entire temperature range, and a DOSY experiment confirmed the exclusive existence of the monomer. In water, variable-temperature experiments and dilution titrations over a wide concentration range initially did not point to any tendency for self-association either, indicated by the constant chemical shifts of all NH protons. However, a 45 mM aqueous solution revealed, on cooling to 275 K, a second set of ^{1}H NMR signals, with significant upfield and downfield shifts for almost all proton signals (Figure 4). A slight signal splitting of the monomer signals in the pyrazole vicinity was observed one week after the sample preparation (see Figure S10, Supporting Information), most likely due to decelerated NH···N tautomer exchange. DOSY measurements with H_2O as the internal standard clearly identify two species of markedly different diffusion rates, the first corresponding to the size of a hexapeptide with a calculated hydrodynamic radius of 8.4 Å, and the other most likely representing the hexameric aggregate, with an R_h value of 15.6 Å (Figure 5).[20] Most of the observed chemical shift changes can be explained by hydrogen bonding (downfield shifts) and π-stacking (upfield shifts); most remarkable, however, are the large downfield shifts in the ethyleneglycol tail, accompanied by a selective downfield shift of lysine's ϵ-methylene group carrying the ammonium functionality. Thus, experimental evidence is provided for the existence of the half-crown complexation motif already found in the crystal structure.

Both the monomeric and hexameric units were examined by means of Karplus analyses[21] and rotating-frame Overhauser

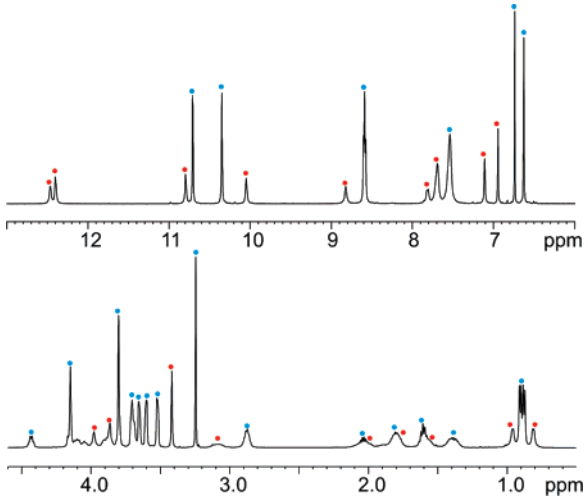

Figure 4. NMR spectrum of monomer and hexamer after cooling to 275 K. Light blue, monomer; red, hexamer signals.

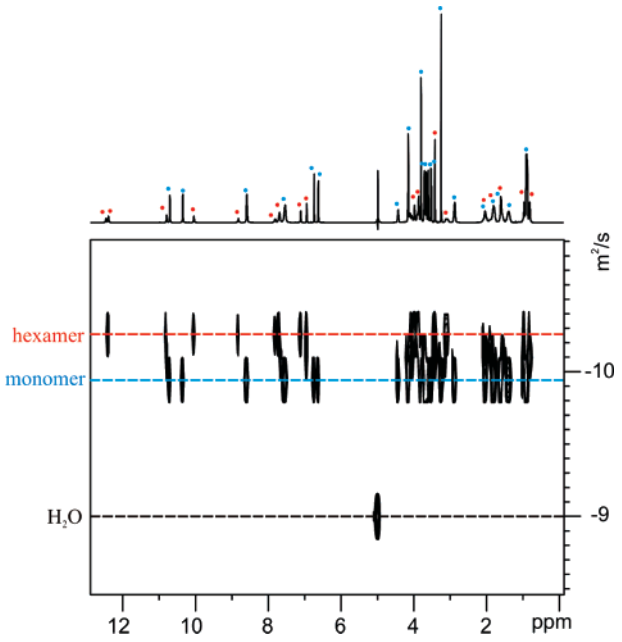

Figure 5. DOSY spectrum for the mixture of monomer and assembly.

enhancement spectroscopy (ROESY) experiments in water. A distinct kink was found in the lysine residue ($^3J_{H,H}$) at higher concentrations, also appearing in valine (ROE). Modeling experiments at the force-field level suggest that intramolecular amide complexation by lysine's NH_3^+ group may be responsible for this unusual conformational preference.[22] Most importantly, the double kink in the peptide bridge serves as a preorganizational force, facilitating the formation of a hydrogen bond network, ultimately leading to the pyrazole rosette. Contrary to the low number of strong intramolecular nuclear Overhauser effect (NOE) contacts in the monomer (Figure 1), a multitude of cross-peaks was found for its higher aggregate. Several of them *must* be intermolecular, since they would surpass the 4.5 Å limit in a monomer unit, regardless of its conformational preference. These characteristic NOE contacts are found between

(18) Kamieth, M.; Klärner, F.-G.; Diederich, F. *Angew. Chem., Int. Ed.* **1998**, *37*, 3303−3306.
(19) Castellano, R. K.; Gramlich, V.; Diederich, F. *Chem. Eur. J.* **2002**, *8*, 118−129.
(20) Johnson, C. S., Jr. *Prog. Nucl. Magn. Reson. Spectrosc.* **1999**, *34*, 203−256. For details of the calculation of R_h, see Supporting Information.
(21) (a) Delepierre, M.; Dobson, C. M.; Poulsen, F. M. *Biochemistry* **1982**, *21*, 4756. (b) Bystrov, V. F. *Prog. Nucl. Magn. Reson. Spectrosc.* **1976**, *10*, 41. (c) Wüthrich, K. *NMR of Proteins and Nucleic Acids*; John Wiley & Sons: New York, 1986; pp 166−168.
(22) MacroModel 7.2, Monte-Carlo simulation, Amber*, water, 5000 steps.

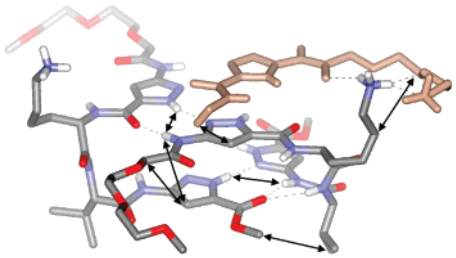

Figure 6. Reciprocal ROESY cross-peaks found in the hexameric aggregate at 275 K (intermolecular contacts). Only two monomers and a fragment of the third are shown for clarity.

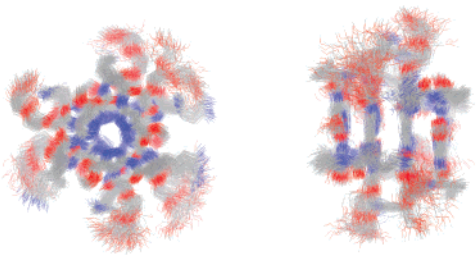

Figure 7. Superimposed snapshots of an MD simulation of the hexameric aggregate (MacroModel 9.0, MMFFs force-field, water, 300 K, 1 ns).

both rosettes and inside the half-crown motif (Figure 6). In spite of its complexity, the whole hexameric aggregate is represented by one single set of NMR signals, due to the characteristic noncovalent head-to-head combination of two C_3-symmetrical trimer units. Dilution weakens the aggregate, as does addition of less polar THF. We tentatively assume that the ethereal solvent effectively competes with the ethyleneglycol tail for ammonium complexation. Polyethers are known for their efficient alkylammonium complexation, relying on multiple ionic NH···O hydrogen bonds.[23] Admittedly, their large negative entropy lowers their cation affinity as opposed to their superior crown ether counterparts.[24] Nevertheless, podands have been successfully used for extraction and transport of chiral ammonium ions through supported liquid membranes.[25] More recently, they found application in oligosaccharide synthesis as podand tags which facilitated affinity separation of the final products on a polymer-supported ammonium ion.[26] This method was even optimized for continuous-flow synthesis in high-throughput saccharide preparation.

Similar to Whiteside's and Reinhoudt's nanorosettes, the aminopyrazole hybrid peptide hexamer is formed with high positive cooperativity—no intermediate oligomer species is observed.[27] The self-assembly process—as well as the dissociation—is also kinetically slow, demonstrated by a sharp new set of ^{1}H NMR signals in water.[28] This may indicate that kinetic control of hydrogen-bonded assemblies with a large number of hydrogen bonds (in our case 54) is also operative in water.[29]

Quantum chemical ^{1}H NMR shift calculations further support the hexameric structure found in solution (see as well the related discussion with respect to molecular tweezers in ref 30). Using a new linear scaling method, NMR chemical shifts were calculated for the monomeric as well as the hexameric aggregate in the gas phase.[31] Intriguingly, the predicted δ values computed in the gas phase agree with those observed in aqueous solution ($\Delta\delta \leq 1.2$ ppm), except for solvent-exposed NH protons. Strong hydrogen bond interactions with the aqueous solvent lead to consistent upfield deviations of 3−4 ppm for all amide and ammonium protons in the monomer. These vanish, however, as soon as the hexamer aggregate is calculated, and the respective protons become engaged in intermolecular hydrogen bonds. Now upfield deviations remain only for the peptidic NH-28 and NH-29, which are solvent-exposed.[32] Thus, further evidence is produced for the pyrazole rosette. Similarly, hydrogen bond formation between lysine's alkylammonium side chain and the oligoethyleneglycol tether diminishes the discrepancy of calculated and observed chemical shifts in CH-15 and NH-31 (Lys) and is also expressed in a downfield shift of almost all half-crown CH-protons, CH-21−26. The experimentally observed conformational lock around each NH_3^+ group is thus independently confirmed by calculation.

Force-field calculations (MacroModel 9.0, water GBA solvation model, MMFFs force-field) were finally used in various solvents (chloroform, water) to study—in a very rough estimation—the thermodynamic stability of the whole hexameric aggregate. Even after minimization (1000 steps), followed by Monte Carlo (2000 steps) and molecular dynamics simulations (1 ns, 300 K), the hexameric aggregate looks very much the same as in the crystal structure, with unaltered dimensions. Thus, its diameters across all the four π-stacks amounts to 9.8 Å; the maximum diameter across one π-face is 24.7 Å (including the half-crown arms), and the minimum diameter across one π-face is 15.4 Å (excluding all half-crowns). In all calculations, the four stacked pyrazole triplets remained intact, and only the half-crown arms moved away from the ammonium cations (Figure 7).

The underlying attractive intermolecular forces bear striking similarity to the self-assembly of nucleic acid double, triple, and quadruple helices. It is instructive to compare the aminopyrazole hexamer to a related peptide nucleic acid (PNA) architecture, since both rely on a peptidic backbone. Much closer to the above-characterized structure than Nielsen's achiral, flexible aminoethylglycine skeleton, utilized in antisense strategies,[33] is the alanyl-PNA, developed in the Diederichsen group (Figure 8).[34] Here, two nucleic bases are indeed bridged by two alanine moieties. As an intended consequence, DNA's dynamic properties are eliminated, and this biooligomer becomes linear, rigid, and well defined. Its linear duplexes have been successfully used to study the influence of artificial nucleobases, pairing

(23) Meot-Ner (Mautner), M.; Sieck, L. W.; Liebman, J.; Schreiner, S. *J. Phys. Chem.* **1996**, *100*, 6445−6450.
(24) Meot-Ner (Mautner), M. *J. Am. Chem. Soc.* **1983**, *105*, 4912−4915.
(25) Martinez-Diaz, M. V.; de Mendoza, J.; Torres, T. *Tetrahedron Lett.* **1994**, *35*, 7669−7672.
(26) Fukase, K.; Takashina, M.; Hori, Y.; Tanaka, D.; Tanaka, K.; Kusumoto, S. *Synlett* **2005**, *15*, 2342−2346.
(27) Mathias, P.; Seto, C. T.; Simanek, E. E.; Whitesides, G. M. *J. Am. Chem. Soc.* **1994**, *116*, 1725−1736.
(28) Mathias, J. P.; Simanek, E. E.; Seto, C. T.; Whitesides, G. M. *Angew. Chem., Int. Ed. Engl.* **1993**, *32*, 1766−1769.
(29) Hasenkopf, B.; Lehn, J.-M.; Boumediene, N.; Leize, E.; Van Dorsselaer, A. *Angew. Chem., Int. Ed.* **1998**, *37*, 3265−3268.
(30) Klärner, F.-G.; Kahlert, B.; Nellesen, A.; Zienau, J.; Ochsenfeld, C.; Schrader, T. *J. Am. Chem. Soc.* **2006**, *128*, 4831−4841.
(31) (a) Ochsenfeld, C.; Kussmann, J.; Koziol, F. *Angew. Chem.* **2004**, *116*, 4585; *Angew. Chem., Int. Ed.* **2004**, *43*, 4485. (b) Kussmann, J.; Ochsenfeld, C. *J. Chem. Phys.* **2007**, *127*, 54103.
(32) The significantly smaller deviation for valine's NH-28 (−2 instead of −3 ppm) indicates its intermolecular hydrogen bond to the aminopyrazole carbonyl group.
(33) Egholm, M.; Buchardt, O.; Nielsen, P. E.; Berg, R. H. *J. Am. Chem. Soc.* **1992**, *114*, 1895−1897. Egholm, M.; Buchardt, O.; Christensen, L.; Behrens, C.; Frier, S. M.; Driver, D. A.; Berg, R. H.; Kim, S. K.; Nordén, B.; Nielsen, P. E. *Nature* **1993**, *365*, 566−568.
(34) Diederichsen, U. *Angew. Chem.* **1996**, *108*, 558−461. Diederichsen, U. *Angew. Chem.* **1997**, *109*, 1966−1969.

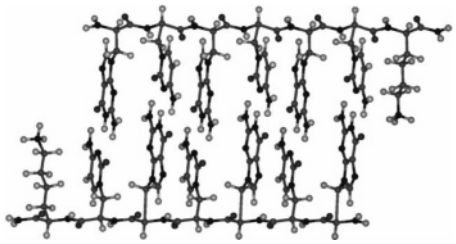

Figure 8. Alanyl-PNA, a closely related architecture.

modes, stacking interactions, and intercalations.[35] Similar to alanyl-PNA, the peptide backbone of our nanorosette holds the pyrazole rings at an exact 3.4 Å distance and dictates "base" orientation and overlap. Helicity is likewise reduced to a minimal degree, producing a rigid, stiff, and well-ordered structure.

In summary, the hybrid peptide **1** is soluble in both organic and aqueous solution, but the assembly is stable in water only at a temperature below 275 K and a concentration surpassing 45 mM. Together with the induced dissociation of the hexamer upon addition of small amounts of THF to an aqueous solution, we conclude that obviously a highly polar environment is the prerequisite for aggregate formation in solution. Taking into consideration the selective weakening of the peripheral half-crown locks in all Monte Carlo and molecular dynamics simulations, experimental evidence has been accumulated for a dominating hydrophobic contribution toward aggregate formation, with π-stacking as the main driving force and *not* hydrogen bond formation. This is indeed an interesting result in light of the ongoing debate on nucleic acid stabilization.

In general, DNA base stacking efficiency is determined by dispersive forces, electrostatics, and solvophobic effects.[36] It is well known that dispersive forces play a crucial role in the gas phase.[37] Replacement of natural nucleosides by nonpolar isosters, developed by Kool et al., further highlighted the importance of efficient stacking, solvophobic, and steric effects for nucleic acid stability and fidelity of DNA replication. Although electrostatic contributions seem to be important for polar natural nucleic acid bases, the most efficient replacements involved nonpolar arenes with large π-faces.[38] Comparative studies between DNA molecules of systematically varied composition revealed a total average stabilization per base pair of ~ -1.4 kcal/mol, with hydrogen bonding accounting for only half of this amount.[39] It will be interesting to compare these results with theoretical calculations on the new nanorosettes presented here. Pyrazoles are small compared to nucleic bases, but the whole nanorosette adopts an area of $\sim$70 Å^2, enough for efficient dispersive attraction. The strong solvent dependence of our nanorosette's thermodynamic stability might as well further emphasize an essential contribution of solvophobic forces and dispersive interactions. Helix formation of flexible aromatic hydrocarbon oligomers, entirely driven by solvophobic forces, has already been observed in water.[40]

Conclusion and Outlook

An artificial hybrid peptide was found to display remarkable features of hierarchical self-assembly in the solid state and in aqueous solution. (1) Subtle sequence-determined structural details lead to an effective preorganization, i.e., a double kink in the peptidic bridging unit. (2) A highly efficient four-fold hydrogen bond pattern between heterocyclic cores establishes a stable rosette, as studied by X-ray, NMR, and quantum chemical calculations. (3) Formation and dissociation of the stacked rosette proceed kinetically slowly. (4) The total absence of detectable intermediate structures underlines the high degree of cooperativity. (5) A strict hierarchical order is maintained throughout the self-assembly process: hydrogen-bonded rosettes induce extensive π-stacking, finished by formation of a six-fold half-crown ammonium lock. (6) The resulting compact assembly is stable in the solid state as well as in aqueous solution. The obtained crystal structure suggests that exchange of valine for a sterically less demanding amino acid might allow infinite extension of stacked rosettes into rosette nanotubes—leading to new fiber-forming materials.[41] It cannot *a priori* be excluded that even higher concentrations or self-assembly of the hybrid peptide **1** on surfaces will eventually lead to head-to-head dimerization of two hexameric aggregates, followed by polymerization into nanofibers.[42] We have modeled the smallest core unit of a potential nanofiber by combining two hexamers at a 60° rotation angle along the main axis in order to release any steric strain from valine's isopropyls. However, even with perfect manual preorientation at a 3.4 Å π-face distance, severe steric strain was produced, which forced both hexameric units to drift apart. No torsion angle was found for the critical isopropyl groups which allowed an energetically favorable stacked arrangement. To clarify this question, atomic force microscopy and transmission electron microscopy experiments are planned for the future, together with dynamic light scattering and UV−vis as well as circular dichroism investigations to complement our ROESY and DOSY studies.

Experimental Section

X-ray Crystallography. Suitable crystals were grown within 4 weeks from a saturated solution in trifluoroacetic acid/diethyl ether ($\sim$1:2 v/v) at −18 °C. Crystal data for $x\cdot 3(C_4H_{10}O)$: $C_{41}H_{74}F_3N_9O_{14}$, $M_r = 974.09$, $0.34 \times 0.33 \times 0.33$ mm^3, trigonal, space group $R32$ (No. 155), $a = 30.9179(10)$ Å, $c = 35.2839(15)$ Å, $V = 29209.7(18)$ Å^3, $Z = 18$, ρ_{cald}=0.997 g cm^{-3}, $F_{000} = 9396$, Mo Kα radiation, $\lambda = 0.71073$ Å, $\mu = 0.080$ mm^{-1}, $T = 120(2)$ K, $2\theta_{max} = 25°$. A total of 63 567 reflections have been collected on a STOE IPDS2 diffractometer; of them, 11 252 were unique ($R_{int} = 0.0724$), 5650 with $I > 2\sigma(I)$ "observed". The structure was solved using the direct methods in SHELXD[43] and refined on F^2 using the full matrix least-squares procedure in SHELXL-97:[44] final R1 = 0.0434 (for the observed

(35) Diederichsen, U. In *Bioorganic Chemistry—Highlights and New Aspects*; Diederichsen, U., Lindhorst, T., Wessjohann, L. A., Westermann, B., Eds.; Wiley-VCH: Weinheim, 1999; pp 255−261. Diederichsen, U.; Weicherding, D.; Diezemann, N. *Org. Biomol. Chem.* **2005**, *3*, 1058−1066.
(36) Pang, Y.-P.; Miller, J. L.; Kollman, P. A. *J. Am. Chem. Soc.* **1999**, *121*, 1717−1725. McKay, S. L.; Haptonstall, B.; Gellman, S. H. *J. Am. Chem. Soc.* **2001**, *123*, 1244−1245.
(37) Sponer, J.; Leszczynski, J.; Hobza, P. *THEOCHEM* **2001**, *573*, 43−53. Sponer, J.; Leszczynski, J.; Hobza, P. *Biopolymers* **2001**, *61*, 3−31.
(38) Kool, E. T.; Morales, J. C.; Guckian, K. M. *Angew. Chem.* **2000**, *112*, 1046−1068.
(39) Kool, E. T. *Annu. Rev. Biophys. Biomol. Struct.* **2001**, *30*, 1−22.
(40) Nelson, J. C.; Saven, J. G.; Moore, J. S.; Wolynes, P. G. *Science* **1997**, *277*, 1793.
(41) Gubala, V.; Betancourt, J. E.; Rivera, J. M. *Org. Lett.* **2004**, *6*, 4735−4738.
(42) Klok, H.-A.; Jolliffe, K. A.; Schauer, C. L.; Prins, L. J.; Spatz, J. P.; Möller, M.; Timmerman, P.; Reinhoudt, D. N. *J. Am. Chem. Soc.* **1999**, *121*, 7154−7155.
(43) Sheldrick, G. M. *SHELXD*; University of Göttingen, Germany, 2002.
(44) Sheldrick, G. M. *SHELXL-97*; University of Göttingen, Germany, 1997.

reflections), GooF = 0.752, wR2 = 0.1001 (for all unique reflections), 411 refined parameters.

The $CF_3CO_2^-$ anion and the ether solvent molecules were not located due to heavy disorder. Therefore, the data set was modified using the "BYPASS (SQUEEZE)" procedure[45] in PLATON.[46] As a result of this procedure, the solvent- and anion-accessible regions of the crystal structure were left as holes by the ordered part of the structure.

The crystallographic data are available in the Supporting Inforamtion for this paper. These data are also deposited as CCDC 638569 and can be obtained free of charge from The Cambridge Crystallographic Data Centre via www.ccdc.cam.ac.uk/data_request/cif.

NMR Spectroscopy. NMR spectra were recorded on a Bruker AVANCE 600 MHz instrument from a 20 mM aqueous solution containing 20 mg of **1** in 0.6 mL of H_2O/D_2O (9:1). After full characterization of the monomer at ambient temperature by ^{1}D, ^{1}H, and ^{13}C NMR, 2D H,H-DQFCOSY, and NOESY (few strong intramolecular cross-peaks), as well as ^{1}H and ^{13}C HSQC and HMBC NMR, a variable-temperature experiment was performed with 5° increments by cooling stepwise from 298 to 270 K. At this temperature, a NOESY experiment was conducted which produced a large number of new intermolecular cross-peaks. In addition, the solvent composition was gradually changed by titration of small amounts of deuterated THF. Pulsed field gradient diffusion experiments were carried out by using the pulse sequence LED-STE on a Bruker Avance-600 spectrometer equipped with a 5 mm broadband inverse probe with Z-gradient (maximum gradient strength 53.5 G/cm). Presaturation was built in the pulse sequence in order to suppress the very strong water signal in the diffusion experiments. The shape of the gradient used was sine, with lengths from 2 to 4 ms. Diffusion delays from 50 to 100 ms were applied. The Bruker software package t1/t2 within TOPSPIN was used to calculate the measured diffusion coefficients. The data were further processed by dosy2d and shown as 2D DOSY plot.

Quantum Chemical NMR Shift Calculations. Force field structure optimizations were performed using Macromodel[47] employing the MMFF94/H_2O force-field.[48] Here, the monomer structure was optimized without constraints, whereas for the hexamer the X-ray structure was taken as a "backbone", and only the hydrogen positions were optimized. All ^{1}H NMR chemical shifts were calculated using the GIAO-HF method[31,49] with the 6-31G** basis set,[50] using 10^{-6} for the self-consistent field (SCF) convergence threshold and 10^{-8} for the integral threshold. Relative shifts were obtained by using a tetramethylsilane molecule as reference, calculated at the same theoretical level. In order to check the reliability of the thresholds employed, test calculations were performed for the monomer structure using tighter thresholds (SCF convergence threshold, 10^{-7}; integral threshold, 10^{-10}), which does not lead to any numerically significant changes in the calculated chemical shifts. All calculations were performed using a development version of the Q-Chem package.[51] Integral contractions have been done using linear-scaling schemes.[52] For the GIAO-HF calculations, our recently developed linear-scaling method was employed, which allows the calculation of NMR shifts with an asymptotically linear-scaling effort for systems with a nonvanishing HOMO−LUMO gap.[31]

In order to check the sufficiency of optimizing hydrogen positions at the force-field level (MMFF94/H_2O), ^{1}H NMR chemical shifts were calculated at the GIAO-HF/6-31G** level, employing the tight thresholds mentioned above, for a monomer structure extracted from the X-ray structure of the hexamer, with hydrogen positions optimized either by force-field or at the B3LYP/6-31G* level[53] using a large grid (Euler−McLaurin/Lebedev−Laikov 75/302[54]) without truncations (for a related comparison of force-field and Hartree−Fock optimization see ref 55). Using these structures, the variations of calculated ^{1}H NMR shifts are typically in the order of 0.1−0.2 ppm and 0.3 ppm at most, indicating that the force-field optimization obviously yields reasonable proton positions for the systems considered.

Acknowledgment. We are indebted to the Volkswagen foundation for funding this project in the priority area "conformational control of biomolecular function". C.O. acknowledges financial support by an Emmy Noether research grant and the "Graduiertenkolleg" GK 441 "Chemie in Interphasen" of the Deutsche Forschungsgemeinschaft. J.Z. thanks the Landesgraduiertenförderung for a graduate fellowship.

Supporting Information Available: Full experimental details, X-ray crystallography, NMR experiments, and quantum chemical shift calculations (PDF, CIF). This material is available free of charge via the Internet at http://pubs.acs.org.

JA0744807

(45) van der Sluis, P.; Spek, A. L. *Acta Crystallogr.* **1990**, *A46*, 194−201.
(46) Spek, A. L. *J. Appl. Crystallogr.* **2003**, *36*, 7−13.
(47) *Macromodel 9.1*; Schrödinger, Inc.: Portland, OR, 2006.
(48) Halgren, T. A. *J. Comput. Chem.* **1996**, *17*, 490.
(49) (a) London, F. *J. Phys. Radium* **1937**, *8*, 397. (b) Häser, M.; Ahlrichs, R.; Baron, H. P.; Weis, P.; Horn, H. *Theor. Chim. Acta* **1992**, *83*, 455. (c) Hameka, H. F. *Mol. Phys.* **1958**, *1*, 203. (d) Ditchfield, R. *Mol. Phys.* **1974**, *27*, 789. (e) Wolinski, K.; Hinton, J. F.; Pulay, P. *J. Am. Chem. Soc.* **1990**, *112*, 8251.
(50) Hariharan, P. C.; Pople, J. A. *Theor. Chim. Acta* **1973**, *28*, 213. Hehre, W. J.; Ditchfield, R.; Pople, J. A. *J. Chem. Phys.* **1972**, *56*, 2257.
(51) Development version of the Q-Chem program package (http://www.q-chem.com).
(52) (a) White, C. A.; Johnson, B. G.; Gill, P. M. W.; Head-Gordon, M. *Chem. Phys. Lett.* **1994**, *230*, 8. (b) Shao, Y.; White, C. A.; Head-Gordon, M. *J. Chem. Phys.* **2001**, *114*, 6572. (c) Ochsenfeld, C.; White, C. A.; Head-Gordon, M. *J. Chem. Phys.* **1998**, *109*, 1663. (d) Ochsenfeld, C. *Chem. Phys. Lett.* **2000**, *327*, 216. (e) Lambrecht, D. S.; Ochsenfeld, C. *J. Chem. Phys.* **2005**, *123*, 184101.
(53) (a) Becke, A. D. *J. Chem. Phys.* **1993**, *98*, 1372. (b) Stephens, P. J.; Devlin, F. J.; Chabalowski, C. F.; Frisch, M. J. *J. Phys. Chem.* **1994**, *98*, 11623.
(54) (a) Murray, C. W.; Handy, N. C.; Laming, G. J *Mol. Phys.* **1993**, *78*, 997. (b) Lebedev, V. I.; Laikov, D. N. *Dokl. Math.* **1999**, *59*, 477.
(55) Zienau, J.; Kussmann, J.; Koziol, F.; Ochsenfeld, C. *Phys. Chem. Chem. Phys.* **2007**, *9*, 4552.